JACS
JOURNAL OF THE AMERICAN CHEMICAL SOCIETY

Communication

pubs.acs.org/JACS

Detection of Electrochemical Reaction Products from the Sodium–Oxygen Cell with Solid-State ^{23}Na NMR Spectroscopy

Zoë E. M. Reeve,[†] Christopher J. Franko,[†] Kristopher J. Harris,[†] Hossein Yadegari,[‡] Xueliang Sun,[‡] and Gillian R. Goward*[,†]

[†]Department of Chemistry and Chemical Biology, McMaster University, 1280 Main Street West, Hamilton, Ontario L8S 4M1, Canada

[‡]Department of Mechanical and Materials Engineering, University of Western Ontario, London, Ontario N6A 5B9, Canada

Supporting Information

ABSTRACT: ^{23}Na MAS NMR spectra of sodium–oxygen ($Na–O_2$) cathodes reveals a combination of degradation species: newly observed sodium fluoride (NaF) and the expected sodium carbonate (Na_2CO_3), as well as the desired reaction product sodium peroxide (Na_2O_2). The initial reaction product, sodium superoxide (NaO_2), is not present in a measurable quantity in the ^{23}Na NMR spectra of the cycled electrodes. The reactivity of solid NaO_2 is probed further, and NaF is found to be formed through a reaction between the electrochemically generated NaO_2 and the electrode binder, polyvinylidene fluoride (PVDF). The instability of cell components in the presence of desired electrochemical reaction products is clearly problematic and bears further investigation.

The sodium–oxygen ($Na–O_2$) battery is an emerging metal–oxygen battery technology that is attracting increasing attention due to its large theoretical energy density coupled with the low cost and high abundance of sodium in nature.[1−3] The design of the $Na–O_2$ battery is analogous to the more widely studied lithium–oxygen ($Li–O_2$) system.[4−8] The $Na–O_2$ cell is comprised of an oxygen reduction electrode, a Na metal anode, and a nonaqueous electrolyte.[9] Molecular oxygen is reduced to the superoxide radical on a carbon support during discharge. In the analogous lithium–oxygen cells, cyclic voltammetry results showing that the superoxide radical is unstable in the $Li–O_2$ system are widely accepted.[10] Lithium superoxide (LiO_2) is initially formed but rapidly undergoes a secondary reduction or disproportionation to lithium peroxide (Li_2O_2).[10,11] In contrast, sodium superoxide (NaO_2) displays increased stability relative to LiO_2, based on both computational[12,13] and experimental results.[14,15] In the $Li–O_2$ system, substantial electrolyte breakdown products, primarily lithium carbonate (Li_2CO_3), were observed. In contrast, less carbonate was found in initial studies of the $Na–O_2$ battery, suggesting that $Na–O_2$ cells offer a cleaner battery chemistry, although the mechanisms of reaction are not well understood and are difficult to control.[14,15]

Sodium superoxide is proposed to be the most electrochemically reversible component and therefore the most desirable reaction product. This would provide the advantage of greater round-trip cycle efficiency by lowering the charging overpotential to <200 mV, if it could be formed exclusively.[15,16] However, NaO_2 has proven to be elusive and potentially unstable,[17] as the electrochemical production of pure NaO_2 has not been unequivocally confirmed in more recent studies.[17−21] Instead, a variety of reaction products including sodium peroxide (Na_2O_2),[22] sodium peroxide dihydrate ($Na_2O_2·2H_2O$),[23] and a mixture thereof[17,18,21] have all been reported as constituent discharge products. Undesirable side products (i.e., sodium acetate, sodium formate, and NaF) have also been reported as minor reaction products.[24,25] Results vary with cell chemistry and the method of detection: PXRD,[18,21,23] Raman,[18,21] IR,[21] TEM,[17,22] SEM,[17,18,21] X-ray absorption near edge structure (XANES),[17] and X-ray photoelectron spectroscopy (XPS).[21,24] The relative ratios and stabilities of these reaction products are not well determined.

We demonstrate here that solid-state nuclear magnetic resonance (ssNMR) spectroscopy; particularly, ^{23}Na NMR, is a valuable diagnostic tool for investigating the $Na–O_2$ battery. ssNMR is an appealing characterization approach for this purpose as it is restricted neither to the surface nor the degree of crystallinity of the electrochemical particles. Instead ssNMR is sensitive to the bulk material and offers element-specific information.

ssNMR has previously been used to investigate $Li–O_2$ batteries.[26−29] In that system, ^{17}O NMR was shown to be a valuable tool for monitoring the discharge products,[26,27] whereas direct 1D ^{6,7}Li NMR spectra were not informative.[28,29]

Unfortunately, ^{17}O NMR studies require expensive and cumbersome isotopic enrichment owing to the low natural abundance of ^{17}O (0.04%), making the widespread use of such a research strategy unlikely. In contrast, ^{23}Na NMR spectra are straightforward to acquire, as the ^{23}Na isotope is 100% naturally abundant and has a favorable magnetogyric ratio, making it an ideal candidate for the characterization of the sodium–oxygen electrochemical reaction products.

^{23}Na magic-angle-spinning (MAS) ssNMR is a well-established technique for studying the molecular structure of inorganic salts and sodium oxide species.[30−33] Sodium (^{23}Na $I = {}^3/_2$) NMR spectra are influenced by not only their chemical shift but also the quadrupole coupling constant.[34] C_q provides structural information as it reflects the environment at the nucleus of interest. This can be appreciated by measurable

Received: October 31, 2016
Published: December 22, 2016

DOI: 10.1021/jacs.6b11333
J. Am. Chem. Soc. 2017, 139, 595−598

differences in the NMR line shapes. It should be noted that the quadrupole interaction causes a field dependence in both the line shape itself and the location of its center of gravity. The ^{23}Na NMR spectra can also be influenced by the paramagnetic interaction, which can add a large frequency shift when unpaired electrons are present in the system, as is the case in NaO_2.[35] Here, a combination of NMR techniques are required to fully characterize the Na−O_2 electrochemical reaction products, due to the differences in local symmetry and electron configuration among these materials. Complementary data from ^{23}Na chemical shifts, relaxation properties, and the quadrupolar interactions of the ^{23}Na nuclei are utilized to identify the electrochemical reaction products produced in Na−O_2 cells.

The ^{23}Na MAS NMR spectra of the relevant electrochemical reaction products are shown in Figure 1. It is immediately

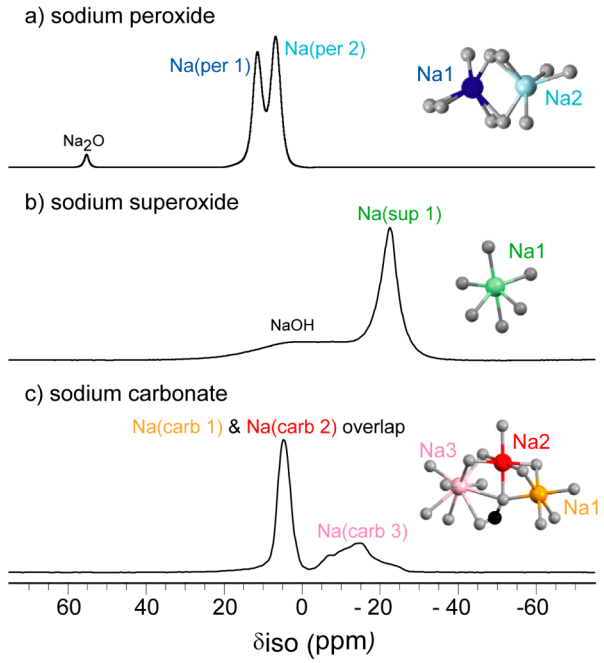

Figure 1. 1D ^{23}Na NMR spectra of (a) sodium peroxide, with a small sodium oxide impurity, (b) sodium superoxide, with residual NaOH, and (c) sodium carbonate. All spectra were collected at room temperature under an MAS frequency of 20 kHz and an 11.7 T applied field. O atoms, gray; C, black; and Na, various colors.

apparent that there is good spectral resolution between these species. Additionally, NaO_2 has a ^{23}Na T_1 relaxation time of 7 ms compared to those of >5 s for sodium peroxide and carbonate. Details of the spectral features and relaxation properties are provided in the Supporting Information and are consistent with previous reports of these phases.[30,36]

For simplicity, ^{23}Na resonances from compounds with multiple crystallographic sites are labeled from high- to low-frequency as $Na_{(comp\text{-}\#)}$, where "comp" indicates the sodium compound. In the case of sodium carbonate, the $Na_{(carb\text{-}3)}$ resonance at low frequency has by far the largest C_q and is therefore assigned to crystallographic site Na3, as it has by far the lowest symmetry in the structure.[37] The other two crystallographic sites are assigned to two overlapping NMR resonances at higher frequency: $Na_{(carb\text{-}1)}$ and $Na_{(carb\text{-}2)}$. The spectral overlap of $Na_{(carb\text{-}1,2)}$ had not previously been resolved and is elucidated in the Supporting Information by applying triple-quantum magic angle spinning (3QMAS).[31,32] In sodium peroxide, the two unique crystallographic Na positions have extremely similar environments, as reflected by their similar NMR parameters. Previously the ^{23}Na NMR data of Na_2O_2 reported a single Na site.[36] 3QMAS provides resolution of the sites; however, they are not definitively assigned due to the similarity of the environments. (See the Supporting Information)

The electrochemical reaction products are determined by examining the extracted Na−O_2 electrodes with 1D and 2D solid-state ^{23}Na MAS NMR. The electrolyte system investigated is a 0.5 M solution of sodium triflate in a standard ether electrolyte, diethylene glycol dimethyl ether (DEGDME). A representative electrochemical curve illustrating the first discharge profile is shown in the Supporting Information. Two samples were selected for the ex situ ^{23}Na NMR study: one early and one later in the discharge process, where the specific capacities were limited to either 100 mAh/g (D_{100}) or 750 mAh/g (D_{750}).

The 1D ^{23}Na NMR spectra of the cycled Na−O_2 electrodes (Figure 2a) illustrate that there is no signal in the sodium superoxide ($Na_{(sup\text{-}1)}$) region at −23 ppm for either discharge capacity. This signifies that NaO_2 is not produced in an appreciable quantity, or, more likely, that NaO_2 is unstable and has been consumed by subsequent reactions. The absence of NaO_2 was confirmed with T_1 filtering experiments, where no evidence of the NaO_2 species was detected, even with many scans at short recycle delays (conditions which enhance the NaO_2 signal while suppressing those of the other species). Rather, one of the sodium peroxide resonances, ($Na_{(per\text{-}1)}$) and one of the sodium carbonate resonances, ($Na_{(carb\text{-}3)}$) are resolved in the 1D NMR spectrum (Figure 2a) at D_{100} and D_{750}. The signal strength increases from D_{100} to D_{750} as an increasing amount of Na-containing reaction products are formed.

Spectral overlap in the multicomponent electrochemical samples can be rectified through 2D ^{23}Na-3QMAS spectroscopy (Figure 2b). ^{23}Na-3QMAS provides spectral resolution of the individual chemical shifts in the indirect (isotropic) dimension and separates the quadrupole lineshapes of each in the direct (isotropic + quadrupolar) dimension (labeled as δ_2 in Figures 2b).[31,32] For example, the 2D ^{23}Na-3QMAS spectrum of D_{750} (Figure 2b) shows clear resolution of all of the five crystallographic Na sites in Na_2O_2 and Na_2CO_3. This 2D 3QMAS spectrum demonstrates that we will be able to successfully separate and identify the electrochemical reaction products and track their presence and quantity as we iterate cell designs. We note sodium has a C_q of 0 in the superoxide, due to the cubic symmetry at the sodium site,[30,38] and is therefore easily identified via its absence in 3QMAS experiments.

An unanticipated species, which we have identified as NaF, is observed at 9 ppm in the 1D ^{23}Na NMR spectra of the cycled electrodes (Figure 2a). The unexpected phase is assigned to NaF owing to the similarity of its ^{23}Na chemical shift to that of pristine NaF (7.4 ppm, Supporting Information). The assignment is additionally supported by filtering out of this new signal in the 3QMAS experiment, as would only be expected for a very high symmetry Na environment such as the cubic salt NaF.[39]

NaF is proposed to result from a reaction between the electrochemically generated superoxide and the polyvinylidene fluoride (PVDF) binder, which acts as a support for the electrode. An analogous reaction, resulting in LiF, is

DOI: 10.1021/jacs.6b11333
J. Am. Chem. Soc. 2017, 139, 595−598

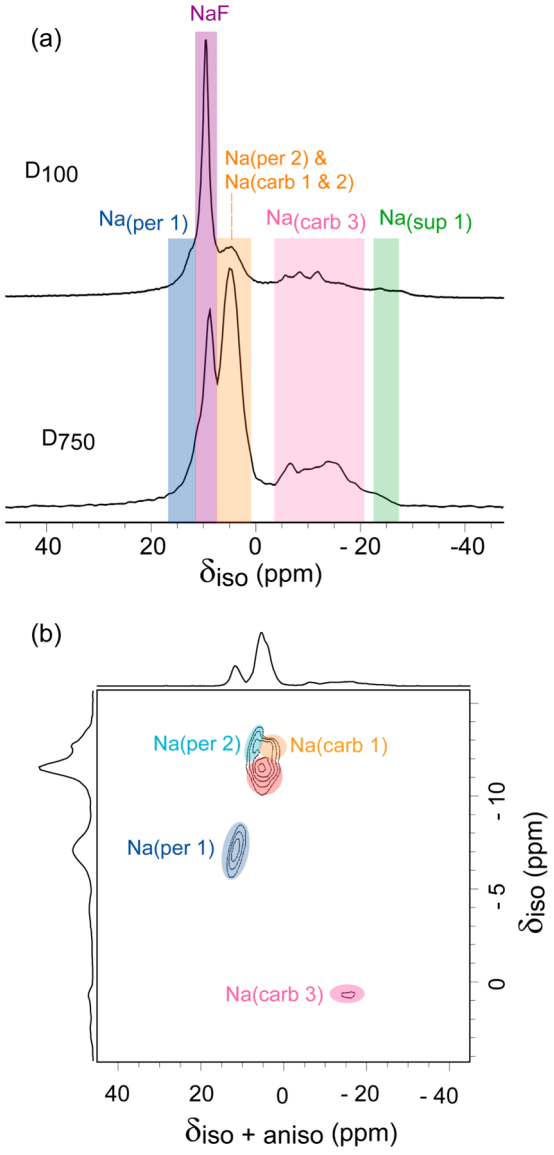

Figure 2. (a) 1D ^{23}Na NMR spectra of cycled electrodes collected at an MAS frequency of 20 kHz at 11.7 T (b) 2D ^{23}Na-3QMAS NMR spectrum of the D_{750} extracted cathode at 11.7 T under 20 kHz MAS.

documented in the Li−O_2 literature.[40] It was unexpected in this case, as the stability of NaO_2 is generally accepted as greater than that of LiO_2,[12−15] though that fact is called into question by these results.

In order to determine the stabilities directly, components of the composite cathode were exposed to the electrochemical reaction products (sodium oxides) and investigated with ^{23}Na NMR; see the Supporting Information for full details. Figure 3a reveals the breakdown products formed by aging a mixture of NaO_2 and Na_2O_2 and a mock cathode (i.e., Super-C65 carbon mixed with PVDF binder) for a week under argon: Na_2CO_3 and NaF are produced, while all NaO_2 and nearly all Na_2O_2 are gone.

The presence of Na_2CO_3 and NaF is confirmed with powder X-ray diffraction of the composite cathode, as discussed in the Supporting Information. We also note that a mixture of NaO_2 and Na_2O_2 aged without the cathode present, as shown in Figure 3b, shows no sign of any reaction. This confirms that NaF and Na_2CO_3 can be generated from solid-state reactions

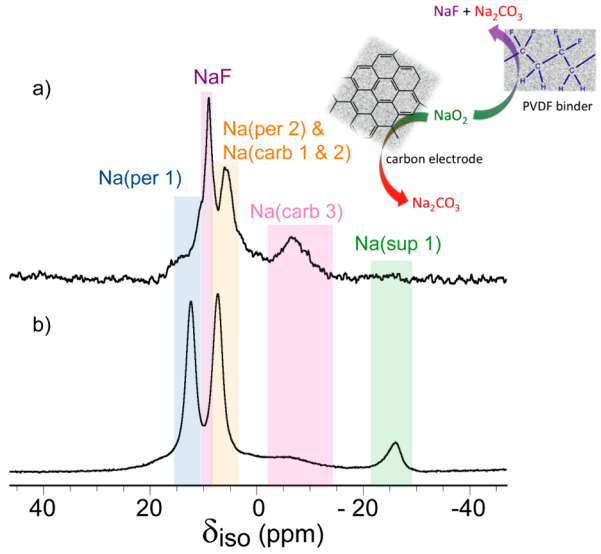

Figure 3. 1D ^{23}Na NMR spectra of (a) a composite cathode where Na_2O_2 and NaO_2 were ground with a carbon + PVDF electrode and (b) a Na_2O_2 and NaO_2 mixture. NMR spectra were collected at 19.9 T under 30 kHz MAS.

involving the discharge products of the Na−O_2 cell and the electrode itself, rather than with the electrolyte as traditionally assumed.[14,41] Both PVDF and Super-C65 carbon are shown to react individually with NaO_2. Details are given in the Supporting Information. Relative roles of electrolyte stability and amorphous carbon/binder stability must therefore be addressed in future studies.

We have shown that ^{23}Na ssNMR is a sensitive probe for unveiling the complex Na−O_2 electrochemistry. With ^{23}Na MAS NMR of Na−O_2 electrodes, expected reaction products Na_2O_2 and Na_2CO_3 are observed in addition to an unanticipated phase, NaF. Both NaF and Na_2CO_3 are observed to result from parasitic reactions involving the carbon electrode and a Na_2O_2/NaO_2 mixture. This demonstrates the reactivity of the Na−O_2 reaction products with the cell components and highlights that Na_2CO_3 may be produced from alternative process other than degradation of the organic electrolyte.

■ ASSOCIATED CONTENT

Supporting Information

The Supporting Information is available free of charge on the ACS Publications website at DOI: 10.1021/jacs.6b11333.

Experimental procedures and supporting data, including ^{23}Na NMR and MQMAS of reference phases, PXRD data, and details of composite electrode reactivity (PDF)

■ AUTHOR INFORMATION

Corresponding Author

*goward@mcmaster.ca

ORCID

Gillian R. Goward: 0000-0002-7489-3329

Notes

The authors declare no competing financial interest.

DOI: 10.1021/jacs.6b11333
J. Am. Chem. Soc. 2017, 139, 595−598

■ ACKNOWLEDGMENTS

We thank K. Neuman and D. Emslie for assistance with the NaO_2 synthesis and V. Jarvis for acquiring PXRD data. G.R.G. acknowledges a supporting NSERC Discovery Grant.

■ REFERENCES

(1) Das, S. K.; Lau, S.; Archer, L. A. *J. Mater. Chem. A* **2014**, *2*, 12623.
(2) Ellis, B. L.; Nazar, L. F. *Curr. Opin. Solid State Mater. Sci.* **2012**, *16*, 168.
(3) Peled, E.; Golodnitsky, D.; Hadar, R.; Mazor, H.; Goor, M.; Burstein, L. *J. Power Sources* **2013**, *244*, 771.
(4) Abraham, K. *J. Electrochem. Soc.* **2015**, *162*, A3021.
(5) Abraham, K.; Jiang, K. *J. Electrochem. Soc.* **1996**, *143*, 1.
(6) Bruce, P. G.; Freunberger, S. A.; Hardwick, L. J.; Tarascon, J.-M. *Nat. Mater.* **2011**, *11*, 172.
(7) Freunberger, S. A.; Chen, Y.; Peng, Z.; Griffin, J. M.; Hardwick, L. J.; Barde, F.; Novak, P.; Bruce, P. G. *J. Am. Chem. Soc.* **2011**, *133*, 8040.
(8) Freunberger, S. A.; Chen, Y.; Drewett, N. E.; Hardwick, L. J.; Bardé, F.; Bruce, P. G. *Angew. Chem., Int. Ed.* **2011**, *50*, 8609.
(9) Sun, Q.; Yang, Y.; Fu, Z.-W. *Electrochem. Commun.* **2012**, *16*, 22.
(10) Peng, Z.; Freunberger, S. A.; Hardwick, L. J.; Chen, Y.; Giordani, V.; Bardé, F.; Novák, P.; Graham, D.; Tarascon, J. M.; Bruce, P. G. *Angew. Chem.* **2011**, *123*, 6475.
(11) Johnson, L.; Li, C.; Liu, Z.; Chen, Y.; Freunberger, S. A.; Ashok, P. C.; Praveen, B. B.; Dholakia, K.; Tarascon, J.-M.; Bruce, P. G. *Nat. Chem.* **2014**, *6*, 1091.
(12) Kang, S.; Mo, Y.; Ong, S. P.; Ceder, G. *Nano Lett.* **2014**, *14*, 1016.
(13) Lee, B.; Seo, D.-H.; Lim, H.-D.; Park, I.; Park, K.-Y.; Kim, J.; Kang, K. *Chem. Mater.* **2014**, *26*, 1048.
(14) McCloskey, B. D.; Garcia, J. M.; Luntz, A. C. *J. Phys. Chem. Lett.* **2014**, *5*, 1230.
(15) Hartmann, P.; Bender, C. L.; Vračar, M.; Dürr, A. K.; Garsuch, A.; Janek, J.; Adelhelm, P. *Nat. Mater.* **2012**, *12*, 228.
(16) Bender, C. L.; Hartmann, P.; Vračar, M.; Adelhelm, P.; Janek, J. *Adv. Energy. Mater.* **2014**, *4*, 1301863.
(17) Yadegari, H.; Banis, M. N.; Xiao, B.; Sun, Q.; Li, X.; Lushington, A.; Wang, B.; Li, R.; Sham, T.-K.; Cui, X.; Sun, X. *Chem. Mater.* **2015**, *27*, 3040.
(18) Kim, J.; Park, H.; Lee, B.; Seong, W. M.; Lim, H.-D.; Bae, Y.; Kim, H.; Kim, W. K.; Ryu, K. H.; Kang, K. *Nat. Commun.* **2016**, *7*, 10670.
(19) Ortiz-Vitoriano, N.; Batcho, T. P.; Kwabi, D. G.; Han, B.; Pour, N.; Yao, K. P. C.; Thompson, C. V.; Shao-Horn, Y. *J. Phys. Chem. Lett.* **2015**, *6*, 2636.
(20) Yadegari, H.; Sun, Q.; Sun, X. *Adv. Mater.* **2016**, *28*, 7065.
(21) Yadegari, H.; Li, Y.; Banis, M. N.; Li, X.; Wang, B.; Sun, Q.; Li, R.; Sham, T.-K.; Cui, X.; Sun, X. *Energy Environ. Sci.* **2014**, *7*, 3747.
(22) Liu, W.; Sun, Q.; Yang, Y.; Xie, J.-Y.; Fu, Z.-W. *Chem. Commun.* **2013**, *49*, 1951.
(23) Kim, J.; Lim, H.-D.; Gwon, H.; Kang, K. *Phys. Chem. Chem. Phys.* **2013**, *15*, 3623.
(24) Hartmann, P.; Bender, C. L.; Sann, J.; Durr, A. K.; Jansen, M.; Janek, J.; Adelhelm, P. *Phys. Chem. Chem. Phys.* **2013**, *15*, 11661.
(25) Black, R.; Shyamsunder, A.; Adeli, P.; Kundu, D.; Murphy, G. K.; Nazar, L. F. *ChemSusChem* **2016**, *9*, 1795.
(26) Leskes, M.; Moore, A. J.; Goward, G. R.; Grey, C. P. *J. Phys. Chem. C* **2013**, *117*, 26929.
(27) Leskes, M.; Drewett, N. E.; Hardwick, L. J.; Bruce, P. G.; Goward, G. R.; Grey, C. P. *Angew. Chem., Int. Ed.* **2012**, *51*, 8560.
(28) Xiao, J.; Hu, J.; Wang, D.; Hu, D.; Xu, W.; Graff, G. L.; Nie, Z.; Liu, J.; Zhang, J.-G. *J. Power Sources* **2011**, *196*, 5674.
(29) Huff, L. A.; Rapp, J. L.; Zhu, L.; Gewirth, A. A. *J. Power Sources* **2013**, *235*, 87.
(30) Krawietz, T. R.; Murray, D. K.; Haw, J. F. *J. Phys. Chem. A* **1998**, *102*, 8779.
(31) Medek, A.; Harwood, J. S.; Frydman, L. *J. Am. Chem. Soc.* **1995**, *117*, 12779.
(32) Frydman, L.; Harwood, J. S. *J. Am. Chem. Soc.* **1995**, *117*, 5367.
(33) Koller, H.; Engelhardt, G.; Kentgens, A. P. M.; Sauer, J. *J. Phys. Chem.* **1994**, *98*, 1544.
(34) Kentgens, A. P. M. *Geoderma* **1997**, *80*, 271.
(35) Grey, C. P.; Dupre, N. *Chem. Rev.* **2004**, *104*, 4493.
(36) Bastow, T. *Z. Naturforsch., A: Phys. Sci.* **1994**, *49*, 320.
(37) Dusek, M.; Chapuis, G.; Meyer, M.; Petricek, V. *Acta Crystallogr., Sect. B: Struct. Sci.* **2003**, *59*, 337.
(38) Ziegler, M.; Rosenfeld, M.; Kaenzig, W.; Fischer, P. *Helv. Phys. Acta* **1976**, *49*, 57.
(39) Dirken, P. J.; Jansen, J. B. H.; Schuiling, R. D. *Am. Mineral.* **1992**, *77*, 718.
(40) Black, R.; Oh, S. H.; Lee, J.-H.; Yim, T.; Adams, B.; Nazar, L. F. *J. Am. Chem. Soc.* **2012**, *134*, 2902.
(41) McCloskey, B. D.; Valery, A.; Luntz, A. C.; Gowda, S. R.; Wallraff, G. M.; Garcia, J. M.; Mori, T.; Krupp, L. E. *J. Phys. Chem. Lett.* **2013**, *4*, 2989.

DOI: 10.1021/jacs.6b11333
J. Am. Chem. Soc. 2017, 139, 595−598